Remimazolam alleviates myocardial ischemia/reperfusion injury and inflammation via inhibition of the NLRP3/IL-1β pathway in mice

XUERU LIU[1*], GUOJING SHUI[1*], YAN WANG[2*], TANGTING CHEN[2,3], PENG ZHANG[2], LI LIU[1], CHUNHONG LI[4], TAO LI[2,3] and XIAOBIN WANG[1]

[1]Department of Anesthesiology, Affiliated Hospital, Southwest Medical University, Luzhou, Sichuan 646000, P.R. China; [2]Key Laboratory of Medical Electrophysiology of The Ministry of Education, Institute of Cardiovascular Research, Southwest Medical University, Luzhou, Sichuan 646000, P.R. China; [3]Department of Cardiology, Affiliated Hospital, Southwest Medical University, Luzhou, Sichuan 646000, P.R. China; [4]Department of Pharmaceutical Sciences, School of Pharmacy, Southwest Medical University, Luzhou, Sichuan 646000, P.R. China

Received July 19, 2024; Accepted November 25, 2024

DOI: 10.3892/ijmm.2025.5498

Abstract. Remimazolam (Rema) is a novel anesthetic that is widely used in anesthesia and sedation in critically ill patients. Notably, Rema exerts effects in patients through activation of the γ-aminobutyric acid (GABA) receptor. GABA may alleviate myocardial ischemia/reperfusion (I/R) injury; however, the impact of Rema and underlying molecular mechanism in myocardial I/R injury remain to be fully understood. Therefore, the present study aimed to investigate the effects of Rema on cardiac I/R injury and to determine the underlying mechanisms. An acute myocardial I/R model was established by ligating the left anterior descending artery in adult male C57BL/6 mice (8-10 weeks). Cultured Raw264.7 cells treated with lipopolysaccharide (LPS) were also used to investigate the effect of Rema on macrophages. The results of the present study revealed that Rema improved I/R-induced cardiac dysfunction by increasing the ejection fraction value and reducing the myocardial infarction area. In addition, Rema also alleviated I/R-induced cardiac inflammatory cell infiltration based on H&E and immunofluorescence staining. Transmission electron microscopy and ROS measurements showed that Rema improved I/R-induced mitochondrial structural disruption and oxidative stress in cardiomyocytes. Transcriptomics analysis and reverse transcription-quantitative PCR revealed that Rema alleviated I/R-induced release of inflammatory factors and cytokines by inhibiting the expression of IL-1β, IL-6, C-C chemokine receptor 2 and C-X-C motif chemokine ligand 5. Rema also inhibited I/R-induced $CD68^+$ cell proliferation, IL-1β release, and NOD-like receptor thermal protein domain associated protein 3 (NLRP3) and IL-1β expression. The results of *in vitro* assays revealed that Rema inhibited LPS-induced increases in IL-1β, IL-6 and TNF-α expression and release in cultured RAW264.7 macrophages. In conclusion, the present study revealed that Rema may alleviate I/R-induced cardiac dysfunction and myocardial injury by inhibiting oxidative stress and inflammatory responses via the NLRP3/IL-1β pathway.

Introduction

Remimazolam (Rema) is a novel intravenous anesthetic agent that activates the γ-aminobutyric acid (GABA) receptor (GABAR), with a fast onset and recovery, and minimal inhibition of cardiopulmonary function (1,2). Rema may exhibit potential in critically ill patients due to the mild cardiac inhibitory effect (3). Notably, anesthesiologists face challenges in protecting vital organs during perioperative periods. Therefore, further investigations are required to explore the pharmacological effects of Rema on organs and tissues other than the brain to elucidate the underlying mechanism, especially in cardiac protection during perioperative periods.

Myocardial ischemia/reperfusion (I/R) injury is a complex pathophysiological process that affects postoperative cardiac function recovery in patients who have undergone cardiopulmonary bypass (CPB) (4,5). When cardiomyocytes are ischemic and damaged, reactive oxygen species (ROS) are activated, and the release of inflammatory cytokines and chemokines such as TNF-α, IL-1, IL-6, C-C chemokine

Correspondence to: Professor Xiaobin Wang, Department of Anesthesiology, Affiliated Hospital, Southwest Medical University, 25 Taiping Street, Jiangyang, Luzhou, Sichuan 646000, P.R. China
E-mail: wangxiaobin67@163.com

Professor Tao Li, Key Laboratory of Medical Electrophysiology of The Ministry of Education, Institute of Cardiovascular Research, Southwest Medical University, 1 Xianglin Road, Longmatan, Luzhou, Sichuan 646000, P.R. China
E-mail: leta49@swmu.edu.cn

*Contributed equally

Key words: myocardial ischemia/reperfusion, remimazolam, oxidative stress, inflammation

receptor 2 (CCR2) and C-X-C motif chemokine ligands (CXCLs) is promoted (6). These factors activate neutrophils and mononuclear macrophages in the blood, infiltrate damaged myocardial cells, and cause microvascular damage, myocardial cell death, extracellular matrix (ECM) degradation and myocardial remodeling, and further promote inflammatory reactions (7). Conversely, the activated inflammatory response further exacerbates oxidative stress, and increases myocardial injury and functional impairment (8). Therefore, inflammation and oxidative stress are key factors in myocardial I/R injury, and may act as key intervention targets for alleviating myocardial I/R injury (9). Further investigations are required for the development of novel treatment options for myocardial I/R injury and the reduction of perioperative cardiovascular complications.

GABA is a central inhibitory neurotransmitter and bioactive small molecule substance that is widely present in peripheral tissue and cells (10). The results of a previous study suggested that GABA may serve a key role in alleviating I/R injury and promoting tissue repair (11). In addition, the results of a previous study suggested that activation of GABAR may inhibit pro-inflammatory activities and promote anti-inflammatory phenotypes in rodent immune cells (12). However, studies focused on the role of GABA or GABAR in myocardial I/R are limited. Wang *et al* (13) previously reported that GABA secreted by the gut microbiome exhibited a cardiac protective effect against I/R injury. A recent clinical study demonstrated that Rema alleviated the surgical stress response in cardiac surgery and adverse cardiac reactions; however, the specific underlying mechanisms are yet to be fully understood (14,15). A previous study has highlighted that GABARs are expressed in macrophages, and GABA/GABAR may exhibit potential as a target for oxidative stress and inflammation regulation (16). Therefore, regulation of GABAR function in macrophages may provide a novel approach for the treatment of cardiac I/R injury.

The present study examined whether the GABAR agonist Rema improves cardiac I/R injury through activation of GABARs in the heart, subsequently inhibiting inflammation and oxidative stress, using a mouse cardiac I/R model and cultured Raw264.7 macrophages. The present study may provide a novel theoretical basis for the use of Rema as an anesthetic in clinical practice.

Materials and methods

Mouse model. Adult male C57BL/6 mice (age, 8-10 weeks; weight, 25.61±1.25 g) were obtained from the Experimental Animal Center at Southwest Medical University (Luzhou, China) for the animal experiments. The present study was approved by the Institutional Animals Ethics Committee at Southwest Medical University, China (ethics approval no. 20221117-011; Luzhou, China) and followed the National Institutes of Health Guide for the Care and Use of Laboratory Animals. All mice used in the present study were maintained at a specific pathogen-free animal center at Southwest Medical University (Luzhou, China) at a constant temperature (25-27˚C) and humidity (45-50%), with a 12 h/light/dark cycle. Mice had free access to sterilized drinking water and food pellets. Mice were anesthetized with 2-5% isoflurane (induction, 5%; maintenance, 2-3%) using a gas anesthesia machine (RWD Life Science Co., Ltd.). The classical method for ligating the left anterior descending coronary artery (LAD) establishes 30-min ischemia and 24-h reperfusion to create a mouse model of left ventricular anterior wall myocardial I/R injury (Fig. 1A) (17). Sham mice underwent thoracotomy without ligation of the LAD. Mice were randomly divided into four groups: i) Sham (n=12); ii) sham + Rema (n=12); iii) I/R (n=18); and iv) I/R + Rema (n=18). Mice were intraperitoneally injected with 15 mg/kg Rema (Jiangsu Hengrui Pharmaceutical Co., Ltd.) following ligation of the LAD for 5 min. Furthermore, 0.9% normal saline was used as the control in the sham and I/R groups. Mice were anesthetized and euthanized immediately after 24 h of reperfusion or sham treatment. Mice were anesthetized using 5% isoflurane followed by cervical dislocation to obtain the heart. A total of 60 mice were used at the beginning in the present experiment. However, there were 4 mice in the I/R and I/R + Rema groups that died unexpectedly during construction of the cardiac I/R model. Finally, 56 mice [Sham (n=12), sham + Rema (n=12), I/R (n=16) and I/R + Rema (n=16)] were used in the final analysis. It is difficult to achieve a 100% survival rate for the cardiac I/R model, even with a skilled laboratory technician (18). The cause of death was pneumothorax or cardiac arrest due to myocardial ischemia.

Echocardiography analysis of intact hearts. Mice were terminally anesthetized using 2-5% isoflurane (induction, 5%; maintenance, 2-3%). Transthoracic M-mode echocardiographic recordings were obtained using the Vevo® 3100 micro-ultrasound imaging system (FUJIFLIM Wako Pure Chemical Corporation) according to the manufacturer's instructions. The ejection fraction (EF) and fractional shortening (FS) were determined using the recorded measurements.

2,3,5-triphenyl tetrazolium chloride (TTC) staining and measurement of the myocardial infarct size. Following 24 h of reperfusion, mice were quickly anesthetized using 5% isoflurane and sacrificed by cervical dislocation, and the injured hearts were obtained. The thoracic cavity of the mice was accessed and 0.5% Evans blue (Sigma-Aldrich; Merck KGaA) was injected into the cardiac apex through reverse perfusion of the aortic root at room temperature, which was kept at -20˚C for 1 h. The heart was cut into 1-mm thickness along the short axis. Heart sections were infiltrated with PBS and subsequently incubated in 1% TTC for 40 min at 37˚C to differentiate the infarcted heart regions. Notably, different colors were indicative of ischemic and non-ischemic areas of the heart. Slices were fixed with 4% polyformaldehyde for 30 min at room temperature. ImagePro Plus 6.0 (Media Cybernetics, Inc.) was used to measure the areas at risk and infarct size.

Transcriptomics array. The transcriptomics array was conducted by Novogene Co., Ltd., according to the manufacturer's instructions. Heart tissues were acquired from each group (sham, 5 mice; sham + Rema, 5 mice; I/R, 9 mice; and I/R + Rema, 8 mice). Total RNA was obtained from each heart tissue with TRNzol Universal Reagent (cat. no: DP424; Tiangen Biotech Co., Ltd.) and the RNA integrity was assessed using the RNA Nano 6000 Assay Kit of the Bio-analyzer 2100

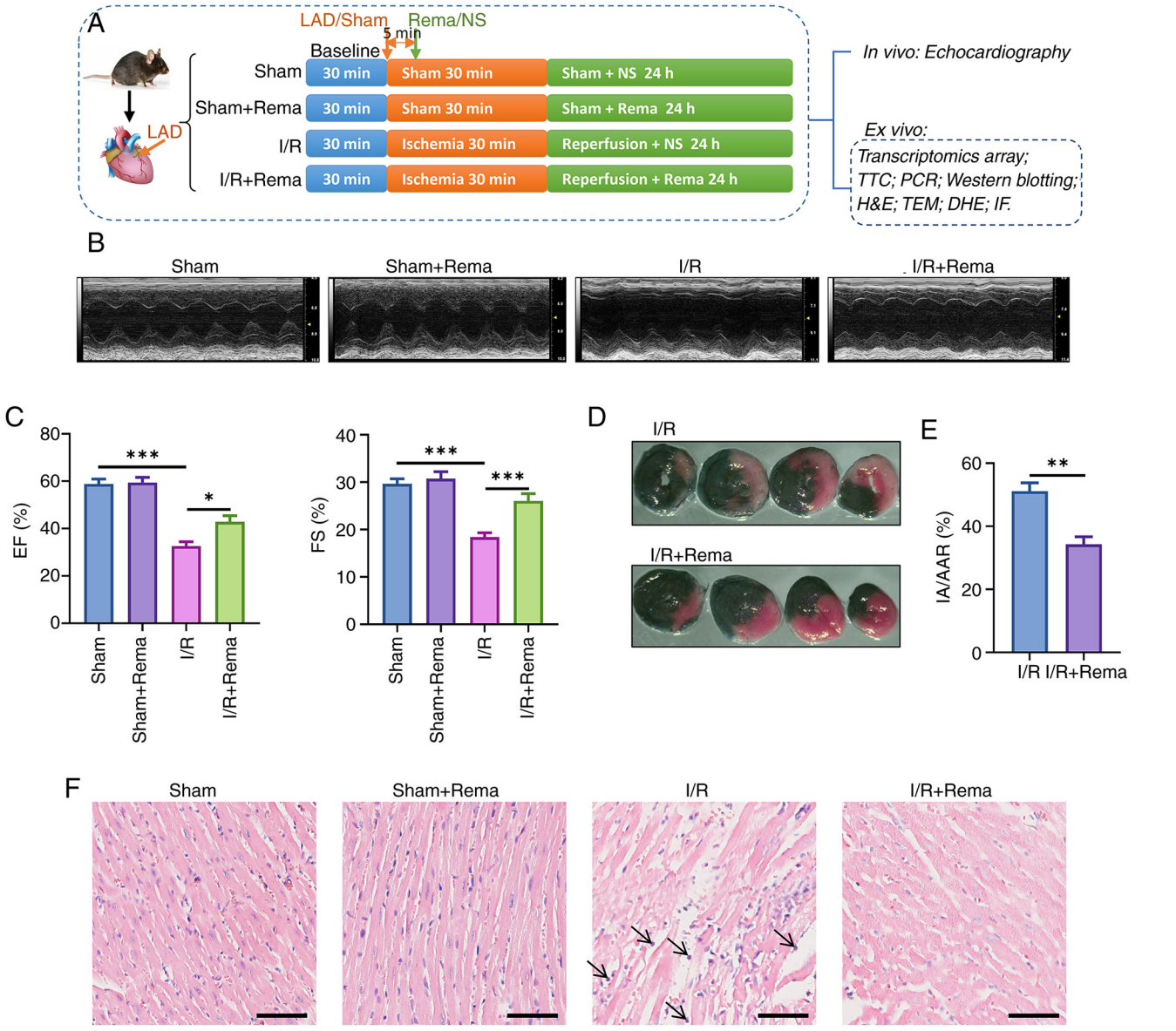

Figure 1. Rema alleviates I/R-induced cardiac injury and dysfunction. (A) Schematic of the experimental design. The I/R model was conducted by ligation of the LAD for 30 min and reperfusion for 24 h. Rema or NS as the control was administered 5 min after LAD. (B) Typical recording of M-type echo in each group. (C) Rema inhibited the I/R-induced decrease of EF and FS values. n=5 mice in the sham and sham + Rema groups; n=8 mice in the I/R and I/R + Rema groups. (D) TTC staining and (E) statistical graph showing that Rema alleviated I/R-induced cardiac infarction by decreasing the cardiac infarction area (n=5). (F) H&E staining showing that Rema alleviated I/R-induced cardiac tissue inflammation. Arrows indicate neutrophil infiltration. Scale bar, 50 μm. *P<0.01; **P<0.01; ***P<0.001. DHE, dihydroethidium; EF, ejection fraction; FS, fractional shortening; IA/AAR, ratio of the infarct area to the area at risk; IF, immunofluorescence; I/R, ischemia/reperfusion; LAD, left anterior descending artery; NS, 0.9% NaCl solution; Rema, remimazolam; TEM, transmission electron microscopy; TTC, 2, 3, 5-triphenyl tetrazolium chloride.

system (cat. no. 5067-1511; Agilent Technologies, Inc.). First strand cDNA was synthesized using random hexamer primers (10 min at 25˚C; 15 min at 42˚C; 15 min at 70˚C; hold at 4˚C) and a library was prepared for transcriptome sequencing with the NEBNext® Ultra™ II RNA Library Prep Kit for Illumina (cat. no. NEB#E7775L; New England BioLabs, Inc.). Clustering of the index-coded samples was performed on a cBot Cluster Generation System using a TruSeq PE Cluster Kit v3-cBot-HS (cat. no. FC-401-3001; Illumina, Inc.). The library preparations [>1.5 nM; measured by reverse transcription-quantitative PCR (RT-qPCR)] were sequenced on an Illumina Novaseq platform (Illumina, Inc.) with the NovaSeq 6000 S4 Reagent Kit v1.5 (300 cycles; cat. no. 20028312; Illumina, Inc.) and 150 base pair paired-end reads were generated. Feature Counts (version 1.5.0; https://subread.sourceforge.net/) was used to count the read numbers mapped to each gene. Data were analyzed with R software (version 3.5.0; https://www.r-project.org/) and Kyoto Encyclopedia of Genes and Genomes (KEGG; https://www.kegg.jp/kegg/pathway.html) for enrichment analysis.

Transmission electron microscopy (TEM). TEM was used to investigate the subcellular structure of heart tissue following different I/R or Rema treatments according to a previously described protocol (19). Briefly, heart tissues were fixed with 3% glutaraldehyde in phosphoric buffer overnight at 4˚C and subsequently fixed with 1% osmate for 1-2 h at 4˚C. Tissues

were dehydrated with gradient alcohol from 30 to 100%, infiltrated with a solution of epoxy resin at room temperature and acetone-embedded in epoxy resin for 24 h at 60˚C. Ultra-thin sections (thickness, 50 nm) were cut and mounted on copper grids, and stained with uranyl acetate for 15 min at room temperature and lead citrate for 2 min at room temperature in the dark. Ultrastructural images were obtained using TEM (JEM-1400PLUS; Japan Electronics Co., Ltd.) at 80 kV.

H&E staining. Hearts from different groups were fixed with 4% polyformaldehyde for 24 h at 4˚C. Cardiac slices were sectioned with 4-μm thickness along the short axis. Routine H&E staining (G1076; Wuhan Servicebio Technology Co., Ltd.) was performed to visualize the overall morphology and structure of myocardial cells at room temperature. The cardiac slices were moved into hematoxylin and stained for 10 min. Subsequently, the slices were moved into water and the hematoxylin and floating color were washed away for 2 min. The differentiation fluid (1% hydrochloric acid alcohol) was added to tissues for differentiation for 30 sec. The slices were moved into water for washing. Eosin was added to the tissues and tissues were stained for 5 min, and then the slices were washed with water. The slices were placed into 95% alcohol for differentiation, and then in anhydrous alcohol for dehydration. Slices were sealed with xylene. Images were acquired using a BX63 automated microscope (Olympus Corporation) under a bright field with a x20 objective lens automatically.

ROS measurement with dihydroethidium (DHE) staining. The superoxide-sensitive dye DHE (cat. no. HY-D0079; MedChemExpress) was used for ROS measurements. Fresh cardiac tissues obtained from the four experimental groups were embedded in Tissue-Tek OCT (Thermo Fisher Scientific, Inc.). Cardiac cross-sections (thickness, 10 μm) were incubated with DHE (10 μM in 0.01% DMSO) at 37˚C for 30 min in a humidified dark chamber. Red DHE fluorescence was detected using an Olympus IX83 fluorescence microscope (Olympus Corporation) at room temperature and analyzed with ImageJ (v1.47; National Institutes of Health).

Immunofluorescence staining. Fresh cardiac tissues from different treatments were embedded in Tissue-Tek OCT (Thermo Fisher Scientific, Inc.). Cardiac cross-sections (thickness, 10 μm) from each group were acquired along the short axis and fixed with 4% polyformaldehyde for 30 min at room temperature. Cardiac sections were treated with 0.1% Triton X-100 for permeabilization for 10 min and blocked with 5% goat serum (G1208; Wuhan Servicebio Technology Co., Ltd.) for 1 h at room temperature. Sections were incubated with primary rabbit anti-CD68 antibody (1:50; cat. no. ab283654; Abcam) or rabbit anti-IL-1β antibody (1:50; cat. no. ab234437; Abcam) at 4˚C overnight. After washing three times (5 min each) with PBS, cardiac sections were incubated with the secondary antibody Goat Anti-Rabbit IgG conjugated with Alexa Fluor® 594 (1:300; cat. no. ab150080; Abcam) for 1 h at room temperature. The nucleus was stained and cardiac cross-section were mounted with undiluted Fluoroshield Mounting Medium with DAPI (cat. no. ab104139; Abcam). Images were acquired on a BX63 automated microscope (Olympus Corporation) with fluorescence (excitation, 590 nm; emission, 617 nm) to scan the whole film under a x20 objective lens automatically and were quantified using ImageJ.

Cell culture. Raw264.7 cells (cat. no. TIB-71; American Type Culture Collection) were cultured in 6-well plates at a density of 1-2x10^5 cells/well for 24 h in DMEM (Gibco; Thermo Fisher Scientific, Inc.) with 10% FBS (Gibco; Thermo Fisher Scientific, Inc.) and 1% penicillin/streptomycin (Gibco; Thermo Fisher Scientific, Inc.). These cells were cultured in a CO_2 incubator with 95% air and 5% CO_2 at 37˚C. Cells were cultured in DMEM without FBS and pre-treated with 100 μg/ml Rema (diluted in DMEM) for 20 min, and subsequently treated with lipopolysaccharide (LPS; 0.5 μg/ml diluted in DMEM; cat. no. HY-D1056H, MedChemExpress) for 24 h in incubator at 37˚C. Cells were cultured in only DMEM without Rema and LPS as the control. After different treatments for 24 h, cells were harvested for RT-qPCR. The culture medium supernatant was collected for ELISAs. In addition, the NOD-like receptor thermal protein domain associated protein 3 (NLRP3) inhibitor dapansutrile (20) (DAPA; 5 μM; cat. no. HY-17629; MedChemExpress) was used with LPS for treatment for 24 h in an incubator at 37˚C.

ELISA. Mouse Uncoated ELISA kits (Shanghai Jianglai Biotechnology Co., Ltd.) were used to determine the protein levels of TNF-α using the Mouse TNF-α ELISA Kit (cat. no. 10484), IL-6 using the Mouse IL-6 ELISA Kit (cat. no. 20268) and IL-1β using the Mouse IL-1β ELISA Kit (cat. no. 18442) in culture medium supernatant from cultured Raw264.7 cells with different treatments using a standard curve according to the manufacturer's instructions. To avoid the influence of cell numbers, the same number of Raw264.7 cells was cultured in each group.

RT-qPCR. Total RNA was isolated from heart tissues or Raw264.7 cells using the RNA Easy Fast Tissue/Cell Kit (cat. no. DP451; Tiangen Biotech Co., Ltd.). Subsequently, total RNA was reverse transcribed into cDNA using ReverTra® Ace qPCR RT Master Mix (cat. no. FSQ-201; Toyobo Life Science) with the following temperature protocol: 37˚C for 15 min, 50˚C for 5 min, 98˚C for 5 min and 4˚C hold. qPCR was performed using Taq Pro Universal SYBR qPCR Master Mix (cat. no. Q712; Vazyme Biotech Co., Ltd.) with an initial denaturation at 95˚C for 30 sec and the following thermocycling conditions: 95˚C for 10 sec, 60˚C for 25 sec and 72˚C for 30 sec for 40 cycles. mRNA expression levels of target genes were normalized to those of GAPDH using the $2^{-\Delta\Delta Cq}$ method (21). The primers used in the present study are shown in Table I.

Western blot analysis. Total protein was extracted from heart tissues using RIPA lysis buffer (Beyotime Institute of Biotechnology). Total protein was quantified using a BCA Protein Assay Kit (Pierce; Thermo Fisher Scientific, Inc.), and 20 μg protein/lane was separated by SDS-PAGE on a 5% stacking gel and 10% separation gel. Separated proteins were subsequently transferred to a PVDF membrane (Millipore, Sigma), which was blocked in Protein Free Rapid Blocking Buffer (1X; cat. no. PS108P, Epizyme; Ipsen Pharma) for 2 h at room temperature. Membranes were incubated with

Table I. Primers for reverse transcription-quantitative PCR analysis of different genes.

Gene	Primer sequence (5'-3')
IL-1β	F: GCAACTGTTCCTGAACTCAACT
	R: ATCTTTTGGGGTCCGTCAACT
IL-6	F: TAGTCCTTCCTACCCCAATTTCC
	R: TTGGTCCTTAGCCACTCCTTC
CCR2	F: ATCCACGGCATACTATCAACATC
	R: CAAGGCTCACCATCATCGTAG
CXCL1	F: AGACTCCAGCCACACTCCAA
	R: TGACAGCGCAGCTCATTG
CXCL5	F: CCTGGTCCGGGATCTTGT
	R: CATGAATGGCGAGATGGAA
CCL12	F: ATTTCCACACTTCTATGCCTCCT
	R: ATCCAGTATGGTCCTGAAGATCA
TNF-α	F: CCCTCACACTCAGATCATCTTCT
	R: GCTACGACGTGGGCTACAG
GAPDH	F:CATCACTGCCACCCAGAAGACTG
	R: ATGCCAGTGAGCTTCCCGTTCAG

F, forward; R, reverse.

primary antibodies against IL-1β (1:1,000; cat. no. ab234437; Abcam), NLRP3 (1:1,000; cat. no. ab270449; Abcam) and β-actin (1:1,000; cat. no. AF0003; Beyotime Institute of Biotechnology) overnight at 4˚C. Following primary antibody incubation, membranes were incubated with HRP-conjugated goat anti-rabbit IgG antibody (1:3,000; cat. no. D110058; Sangon Biotech Co., Ltd.) or HRP-conjugated goat anti-mouse IgG antibody (1:3,000; cat. no. D110087; Sangon Biotech Co., Ltd.) for 1 h at room temperature. Membranes were incubated with chemiluminescent HRP substrate (MilliporeSigma) at room temperature for 30 sec. Images were obtained using the Universal Hood II System (Bio-Rad Laboratories, Inc.) and analyzed using ImageJ.

Statistical analysis. Continuous data are presented as the mean ± SEM and were analyzed using two-way ANOVA followed by the Sidak test for further multiple group comparisons (GraphPad Prism 9.0; Dotmatics). For two groups, differences were evaluated using an unpaired Student's t-test. $P<0.05$ was considered to indicate a statistically significant difference.

Results

Rema alleviates I/R-induced cardiac dysfunction. In the present study, cardiac function was evaluated by echocardiography *in vivo* (Fig. 1B and C). The results demonstrated that EF values decreased from 58.84±2.09% (sham group) to 32.65±1.67% (I/R group), highlighting that I/R significantly inhibited cardiac function. In addition, EF values increased to 42.90±2.39% (I/R + Rema group) following treatment with Rema, highlighting that Rema significantly inhibited I/R-induced cardiac dysfunction. Notably, the impact of Rema on FS was comparable (Fig. 1B), with levels increasing from 18.42±0.84% to 26.05±1.44% (n=8; $P<0.05$).

The results of the TTC staining assay revealed minimal areas of infarction in the sham and sham + Rema groups (Fig. S1); however, the cardiac infarct area (IA) in the I/R group was increased (Fig. 1D). Notably, treatment with Rema markedly decreased the infarction area compared with that in the I/R group, as the ratio of the IA to the area at risk shifted from 51.11±2.66% to 34.29±2.36% (n=5; $P<0.01$; Fig. 1D and E).

The results of the H&E staining assay revealed that, in the I/R group, cardiomyocytes and myocardial fibers were arranged in a disordered manner (Fig. 1F). In addition, some myocardial fibers showed interstitial edema and inflammatory neutrophil infiltration, which are indicated by black arrows. Following treatment with Rema, structural damage and inflammatory cell infiltration of myocardial tissues were alleviated. Notably, treatment with Rema alone did not affect the myocardial structure.

Rema alleviates I/R-induced mitochondrial structural disruption and oxidative stress. Inflammation and oxidative stress are key pathological and physiological processes in cardiac I/R injury (6,7). Thus, the effects of Rema on I/R-induced subcellular structural disruption of myocardial tissues were evaluated using TEM and ROS levels were evaluated using DHE staining (Fig. 2). Notably, mitochondria are a key source of oxidative stress and ROS production (8). The results of the present study demonstrated that I/R injury caused disordered arrangement of the cardiac cell structure, including swelling of the mitochondrial structure and vacuoles, while treatment with Rema improved the I/R-induced structural abnormalities of cardiomyocytes (Fig. 2A). DHE staining demonstrated that I/R significantly induced ROS production, while Rema significantly alleviated I/R-induced ROS production (n=5; Fig. 2B and C). Notably, the mitochondrial structure and ROS levels in the sham group were not impacted following treatment with Rema.

Transcriptomics arrays may highlight the underlying signaling pathway. To further explore the mechanisms underlying the alleviation of cardiac I/R injury following treatment with Rema, a transcriptomics array was carried out using heart tissues (Fig. 3). A heatmap of gene clusters in each group is shown in Fig. 3A. The results of the present study revealed that I/R injury induced alterations in gene clusters, while treatment with Rema partially reversed these I/R-induced changes in gene cluster. KEGG enrichment analysis of differentially expressed genes (DEGs; $P<0.05$ and $\log_2$ fold change >1) demonstrated that DEGs were enriched in pathways such as 'cytokine-cytokine receptor interaction' and 'ECM-receptor interaction' (Fig. 3B). Following treatment with Rema, DEGs were enriched in pathways such as 'cell cycle' and 'ECM-receptor interaction'. DEGs that were notably upregulated or downregulated were further analyzed, and the results revealed that I/R induced upregulation of 820 DEGs and downregulation of 431 DEGs. Notably, the 820 upregulated DEG were enriched in inflammatory pathways, including the 'TNF signaling pathway' and 'chemokine signaling pathway', and in 'cytokine-cytokine receptor interaction' and 'ECM-receptor interaction'. Following treatment with Rema, 108 DEGs were

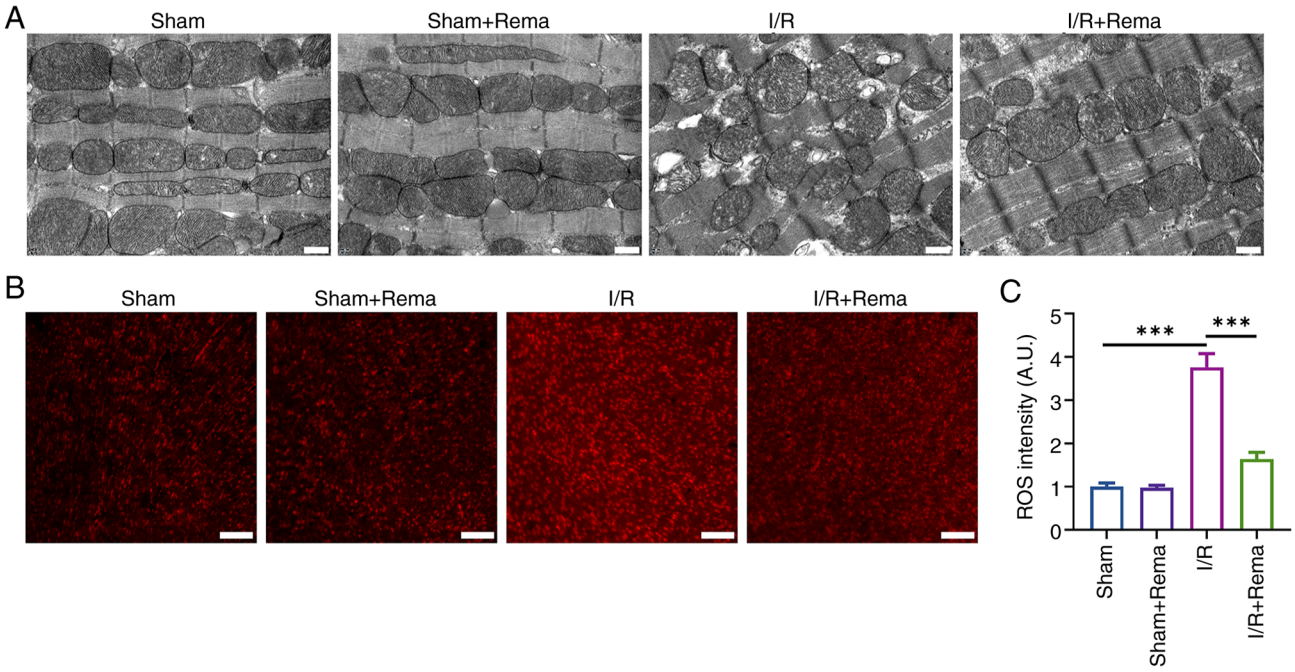

Figure 2. Rema alleviates I/R-induced alterations of cardiac mitochondrial structure and oxidative stress. (A) Transmission electron microscopy showing I/R-induced mitochondrial structural disorder of cardiomyocytes and that Rema reversed the I/R-induced disorder. Scale bar, 500 nm. (B) Dihydroethidium staining showing that I/R increased ROS levels and that Rema inhibited the effects of I/R. Scale bar, 100 μm. (C) Statistical graph showing that Rema inhibited the I/R-induced increase in ROS intensity (n=5). ***P<0.001. A.U., arbitrary units; I/R, ischemia/reperfusion; Rema, remimazolam; ROS, reactive oxygen species.

upregulated and 195 DEGs were downregulated. Notably, the 195 downregulated DEGs were enriched in 'ECM-receptor interaction'.

Collectively, these results suggested that Rema may exert effects on I/R injury via the inflammatory pathway. Thus, the heatmap showed the expression levels of the main genes involved in inflammatory, cytokine or chemokine pathways in Fig. 4A, and these were analyzed using RT-qPCR (Fig. 4B and C). The I/R-induced increases of the expression levels of CXCL1, CXCL5, CCR2, CC motif chemokine ligand 12 (CCL12), IL-1β, IL-6 and TNF-α were reduced following treatment with Rema (n=5). These results further demonstrated that Rema may exert protective effects on I/R injury via the regulation of genes involved in inflammatory, cytokine or chemokine pathways.

Rema protects against I/R-induced cardiac injury via NLRP3/IL-1β. The activation of macrophages is the key pathophysiological process in cardiac I/R injury (22). I/R causes an inflammatory response and activated macrophages are recruited to myocardial tissue (23). Thus, the activation of macrophages was determined in the present study using immunofluorescence staining of CD68, which is expressed in macrophages (Fig. 5A). Notably, the results of the present study revealed that I/R injury significantly increased the number of $CD68^+$ cells, while treatment with Rema inhibited I/R-induced $CD68^+$ cell proliferation. As CD68 is expressed in macrophages and is widely found in circulating blood, the present study showed that there was some overlap between the red fluorescence signal and cardiomyocytes (Fig. 5A). This may be due to CD68 staining with red fluorescence overlapping with cardiomyocytes as a few macrophages infiltrated the myocardial tissue.

NLRP3, a key inflammatory regulatory factor, serves a role in myocardial cell inflammation through the activation of downstream inflammatory factor release, thereby causing myocardial damage. Thus, NLRP3 is a key treatment target in I/R injury (24). In the present study, the expression levels of IL-1β were examined using immunofluorescence staining, and NLRP3 and IL-1β expression was evaluated using western blotting (Fig. 5). The results of the present study demonstrated that I/R injury significantly increased the fluorescence intensity of IL-1β, while treatment with Rema inhibited I/R-induced IL-1β expression (n=3; P<0.01; Fig. 5B). In addition, the protein expression levels of NLRP3 and IL-1β were increased following I/R, while treatment with Rema reversed the I/R-induced alterations in NLRP3 and IL-1β expression (n=4; Fig. 5C and D). Notably, treatment with Rema alone did not impact NLRP3 and IL-1β expression. Collectively, these data suggested that Rema may protect against I/R-induced cardiac injury via NLRP3/IL-1β.

Rema inhibits the LPS-induced inflammatory response in RAW264.7 cells. In the present study, the effects of Rema (100 μg/ml) on the LPS-mediated expression of inflammatory factors were evaluated using cultured RAW264.7 cells (Fig. 6). The release of IL-1β, IL-6 and TNF-α in the cell supernatant was detected using ELISAs. LPS increased the expression levels of IL-1β, IL-6 and TNF-α to 1,668.66±89.35, 490.57±12.49 and 2,904.05±194.51 pg/ml, respectively. Following treatment with Rema, the expression levels of IL-1β, IL-6 and TNF-α were reduced to 773.04±28.19, 177.25±8.62 and 756.64±48.08 pg/ml, respectively (n=3; Fig. 6B). Furthermore, RT-qPCR analysis revealed that LPS treatment increased the relative expression levels of IL-1β, IL-6 and TNF-α 232.89±8.16, 71.99±7.75 and

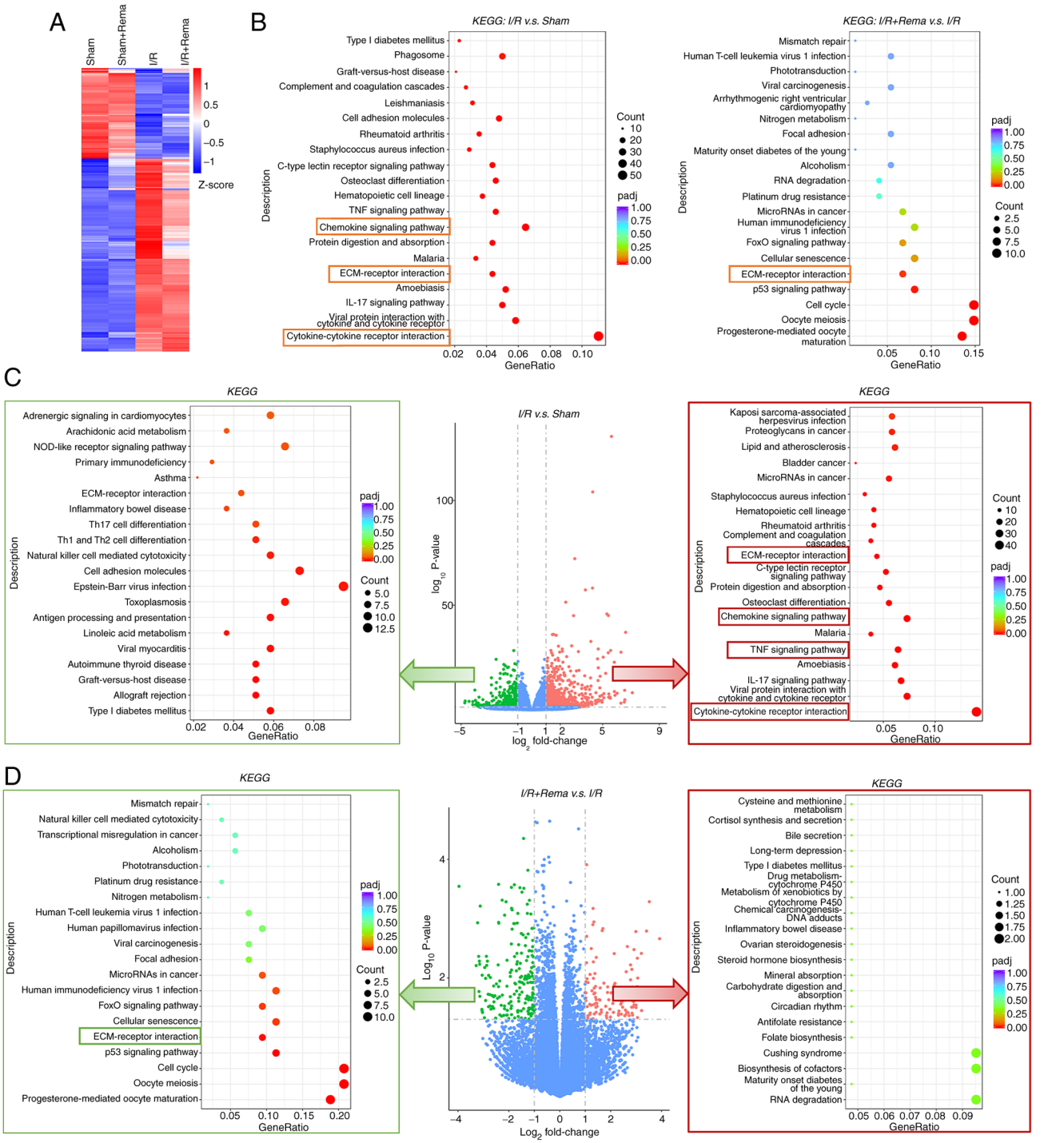

Figure 3. Transcriptomics arrays showing that Rema exerts effects on I/R-induced cardiac injury via specific signaling pathways. (A) Heatmap of gene clusters in each group. I/R treatment induced changes in gene clusters, while Rema partially reversed the I/R-induced changes. The level of gene expression was standardized using the Z-score. (B) KEGG enrichment analysis of DEGs (P<0.05 and $\log_2$ fold change >1) for I/R vs. sham and I/R + Rema vs. I/R showing the top 20 pathways. (C) Volcano plot (middle panel) revealing that I/R induced the upregulation of 820 DEGs and the downregulation of 431 DEGs. The 820 upregulated DEGs were enriched in inflammatory pathways, including the 'TNF signaling pathway' and 'chemokine signaling pathway', and in 'cytokine-cytokine receptor interaction' and 'ECM-receptor interaction' (right panel with red frame). (D) Volcano plot (middle panel) revealing that Rema induced the upregulation of 108 DEGs and the downregulation of 195 DEGs. The 195 downregulated DEGs were enriched in 'ECM-receptor interaction' (left panel with green frame). Pathways highlighted with red and green boxes are inflammatory and inflammation-related pathways. n=5 in the sham and sham + Rema groups; n=9 in the I/R group; n=8 in the I/R + Rema group. Ctrl, control; DEGs, differentially expressed genes; ECM, extracellular matrix; I/R, ischemia/reperfusion; KEGG, Kyoto Encyclopedia of Genes and Genomes; padj, adjusted P-value; Rema, remimazolam.

17.57±1.63 times compared with the control group, respectively. Notably, treatment with Rema reduced the relative expression levels of IL-1β, IL-6 and TNF-α 51.51±3.02, 13.12±0.63 and 2.77±0.23 times compared with the LPS group, respectively (n=3; Fig. 6C). In addition, Rema treatment did not significantly affect the effects of the NLRP3 inhibitor DAPA (5 μM) on LPS-induced release of IL-1β, IL-6 and TNF-α in the Raw264.7 cell supernatant (n=3; Fig. 6D).

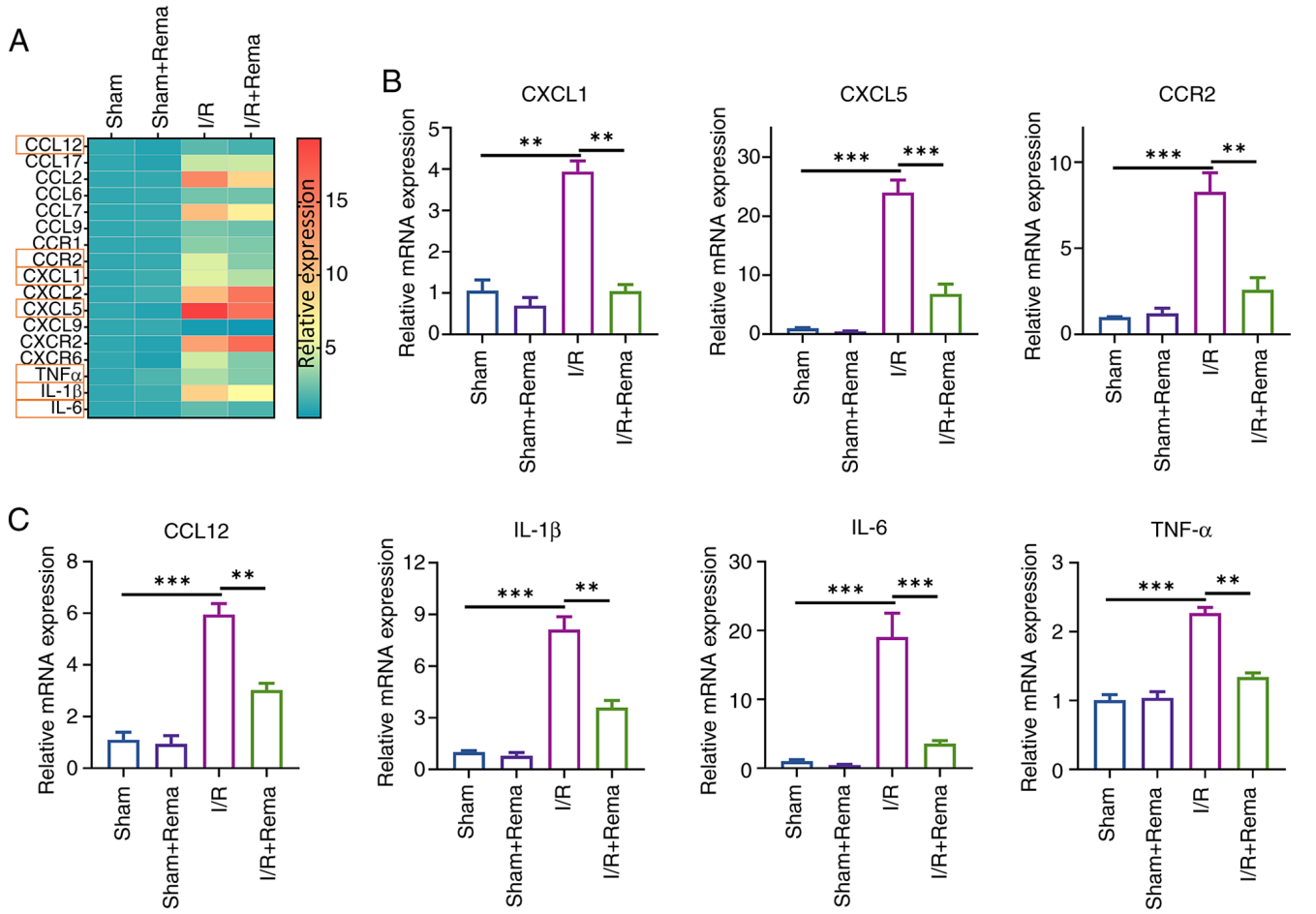

Figure 4. Rema exerts effects on I/R injury via inflammatory molecules and chemokines. (A) Heatmap of inflammatory molecules and chemokines following treatment with Rema. The red boxes indicate the seven selected molecules that were further confirmed by reverse transcription-quantitative PCR. The relative expression of each gene was normalized to the value in the sham group. (B) Statistical graphs showing that Rema inhibited the I/R-induced alterations in CXCL1, CXCL5 and CCR2. (C) Statistical graphs showing that Rema inhibited the I/R-induced alterations in CCL12, IL-1β, IL-6 and TNF-α. n=3 in the sham and sham + Rema groups; n=5 in the I/R and I/R + Rema groups. **P<0.01; ***P<0.001. CCL, C-C motif chemokine ligand; CCR, C-C chemokine receptor; CXCL, C-X-C motif chemokine ligand; CXCR, C-X-C motif chemokine receptor; I/R, ischemia/reperfusion; Rema, remimazolam.

Discussion

As a novel intravenous anesthetic agent, Rema differs from alternate conventional anesthetics, with a rapid onset, recovery and metabolism (2). According to the metabolic pathways, Rema is rapidly metabolized by tissue esterase to an inactive carboxy acid metabolite, and the related clinical research also showed that Rema has no accumulation effects following long-term use (25,26). Rema has been used in clinical practice for several years since 2020 (27). More clinical studies and clinical cases regarding addictive behaviors or unpredicted mental effects, especially in long-term use of Rema, should be performed and reported. The results of previous clinical studies have revealed that Rema exhibits stable hemodynamics in critically ill patients, without causing a dose-dependent blood pressure reduction (3,14,15). Thus, the present study focused on the impact of Rema on cardiac I/R injury. The results first demonstrated that Rema inhibited cardiac I/R injury by attenuating I/R-induced inflammation and oxidative stress via the NLRP3/IL-1β pathway. Therefore, the present study provides a novel theoretical basis for the use of Rema in clinical practice, particularly in cardiac surgery.

I/R injury is the main pathophysiological process leading to cardiac injury in ischemic heart diseases, and one of the main causes of postoperative cardiac dysfunction and death in critically patients who have undergone cardiac surgery (28-30). Notably, anesthetic agents that exert cardioprotective effects in patients may be more beneficial in this context (31,32). The results of previous studies have revealed that numerous intravenous anesthetic agents, including propofol, dexmedetomidine and etomidate, exert cardioprotective effects (33-35). However, these agents may also cause adverse effects in patients, including inhibition of the circulatory system, leading to hypotension (36). Thus, the development of novel anesthetic agents with few adverse effects is required. Notably, Rema exerts similar anesthetic effects as propofol. Rema acts on GABARs in the central nervous system; however, the involved metabolic pathways differ from those required by propofol (37). The results of the present study demonstrated that Rema inhibited I/R-induced myocardial injury in mice, highlighted by improved cardiac function and decreased myocardial infarction. Thus, the cardiac protective effects of Rema may facilitate its use in clinical practice.

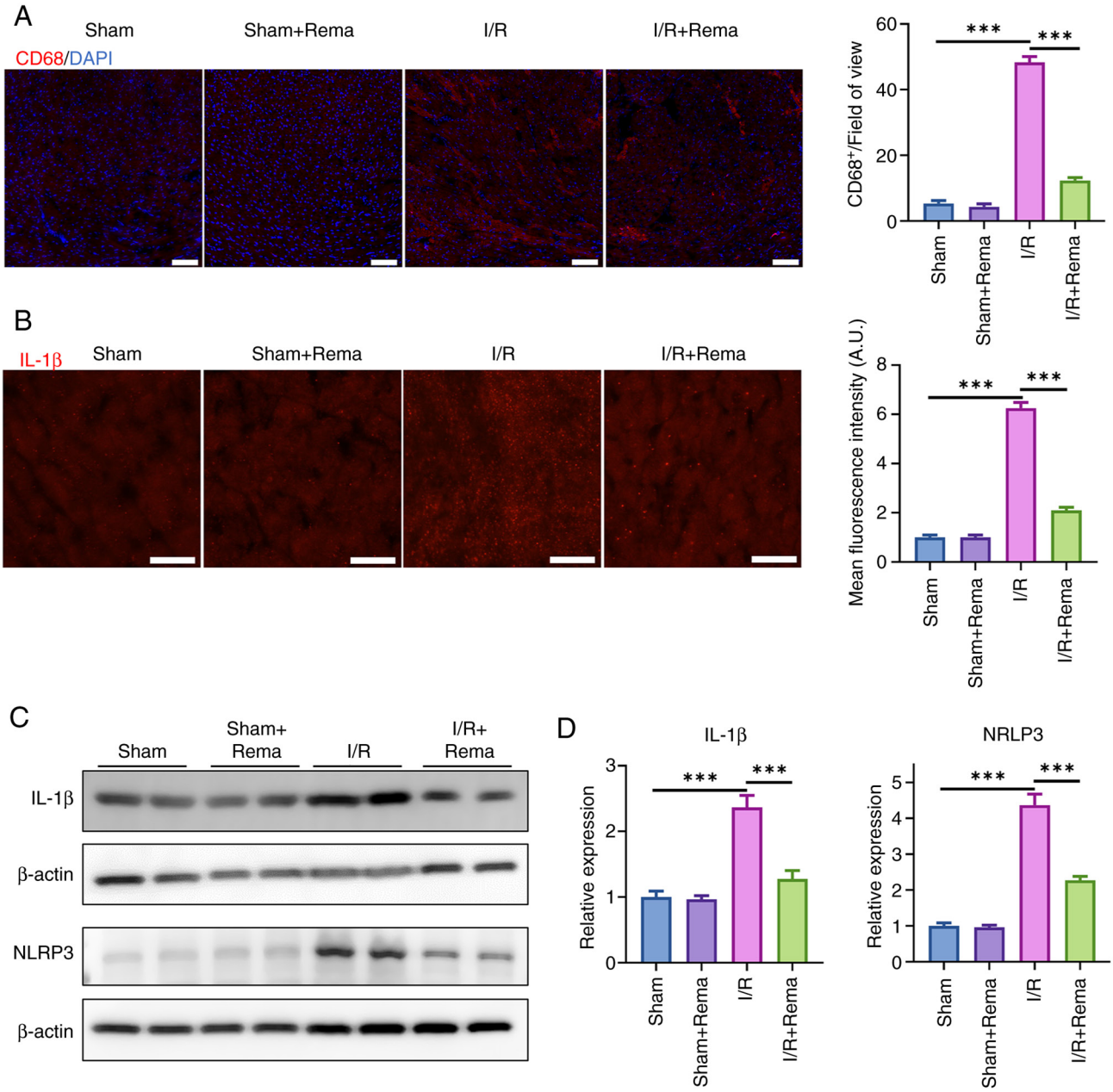

Figure 5. Rema alleviates I/R-induced inflammation and activation of NLRP3/IL-1β. (A) Rema inhibited I/R-induced CD68+ cell (red) proliferation and infiltration. The statistical graph showed that Rema inhibited CD68+ cell proliferation induced by I/R injury (n=3). Scale bar, 100 μm. (B) Effects of Rema on the expression levels of IL-1β (red) were evaluated using immunofluorescence staining. The statistical graph showed that Rema inhibited I/R-induced alterations in IL-1β expression (n=3). Scale bar, 20 μm. (C) Representative images showing that Rema inhibited I/R-induced alterations in NLRP3 and IL-1β expression. (D) Statistical graphs showing that Rema inhibited the I/R-induced increase in expression of NLRP3 and IL-1β (n=4). ***P<0.001. A.U., arbitrary units; I/R, ischemia/reperfusion; NLRP3, NOD-like receptor thermal protein domain associated protein 3; Rema, remimazolam.

Inflammation and oxidative stress are key mechanisms underlying I/R injury (38,39). The results of the present study revealed that Rema effectively suppressed I/R-induced elevation of inflammation levels and oxidative stress. Further transcriptomics analysis and RT-qPCR demonstrated that Rema exerted cardioprotective effects through cytokines, chemokines and the ECM. In addition, the NLRP3 inflammasome serves a role in myocardial I/R injury (40,41), exhibiting potential as a treatment target (24,42). Thus, the effects of Rema on NLRP3 inflammasome activation and the downstream secretion of IL-1β were examined in the present study. The results demonstrated that Rema significantly inhibited the I/R-induced increase in the expression levels of NLRP3 and IL-1β. The results of the transcriptomics analysis may also provide a basis for understanding the mechanisms underlying the additional effects of Rema in cardiac I/R injury.

Macrophages are key cells involved in the inflammatory response of the heart and are key intervention targets for cardiovascular diseases (22). Previous studies have revealed that GABARs were not expressed in cardiomyocytes; however, these were expressed in macrophages (16,43). The results of the present study revealed that treatment with Rema significantly inhibited the increase in CD68+ cells induced by I/R, indicating that macrophages may be involved in the protective

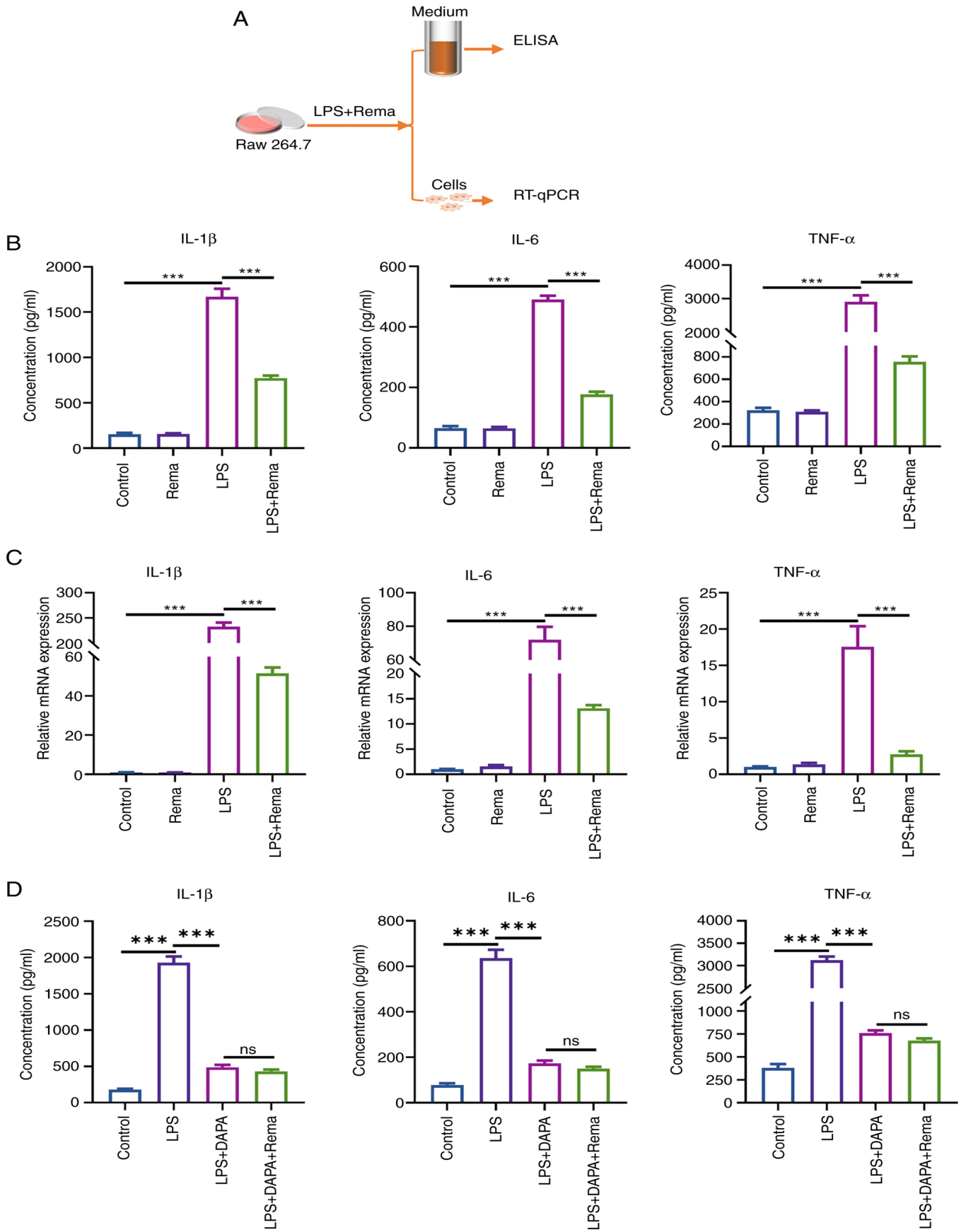

Figure 6. Rema alleviates LPS-induced release and increased expression levels of IL-1β, IL-6 and TNF-α in cultured Raw264.7 cells. (A) Experimental protocol using cultured Raw264.7 macrophages. (B) LPS induced alterations in the release of IL-1β, IL-6 and TNF-α in Raw264.7 cells, while treatment with Rema inhibited these LPS-mediated changes (n=3). (C) LPS induced alterations in the gene expression levels of IL-1β, IL-6 and TNF-α in Raw264.7 cells, while treatment with Rema inhibited these effects (n=3). (D) DAPA inhibited the LPS-induced release of IL-1β, IL-6 and TNF-α in Raw264.7 cells, while treatment with Rema did not affect the alterations induced by DAPA (n=3). ***P<0.001. DAPA, dapansutrile; LPS, lipopolysaccharide; ns, not significant; Rema, remimazolam; RT-qPCR, reverse transcription-quantitative PCR.

effects of Rema against I/R injury. In addition, Rema significantly inhibited LPS-induced increases in IL-1β, IL-6 and TNF-α expression and secretion. Collectively, these results may indicate that Rema inhibited the LPS-induced inflammatory phenotype of macrophages, leading to reduced cardiac inflammation during I/R injury. The results of a previous study have revealed that propofol, a similar intravenous anesthetic activating GABAR, regulated inflammation by modulating macrophage migration, recruitment, polarization and pyroptosis (44). However, research regarding macrophages in the effects of propofol on cardiac I/R injury is also limited.

The present study has limitations. The present study revealed that macrophages may serve important roles in the cardiac protective effects of Rema against I/R injury. However, the direct effect of Rema on cardiomyocytes was not investigated in the present study. The results of previous studies have revealed that propofol exerted a direct cardioprotective effect in cultured neonatal myocardial cells treated with H_2O_2 (33,45). Although GABAR is not expressed in cardiomyocytes, Rema may affect cardiomyocytes directly through other mechanisms. Thus, whether Rema also exerts a direct effect on cardiomyocytes and alleviates oxidative stress-induced myocardial cell damage independent of GABARs also remains unknown. Further investigations should focus on the use of cell co-culturing to further investigate the direct and indirect effects of Rema in cardiomyocytes. Further investigations may reveal the cellular and molecular mechanisms underlying the effects of Rema in the heart. These investigations will further expand the understanding of cardiac protective effects of Rema and other anesthetics acting through GABAR.

In conclusion, the present study systematically investigated the effects of Rema on I/R-induced cardiac injury and the specific underlying mechanisms. The results of the present study revealed that Rema may inhibit I/R-induced inflammation and oxidative stress. The present study provides a novel theoretical basis for the use of Rema in clinical practice, with potential for beneficial outcomes in patients who experience cardiac I/R injury during CPB.

Acknowledgements

Not applicable.

Funding

The present study was supported by the National Natural Science Foundation of China (grant no. 31900813), Sichuan Science and Technology Program, China (grant nos. 2022YFS0632, 2022YFS0627, 2023ZYD0093 and 2024NSFSC0305) and Bureau of Science and Technology of Luzhou (grant no. 2024JYJ006).

Availability of data and materials

The RNA sequencing data generated in the present study may be found in the BioProject database of the National Library of Medicine under accession number PRJNA1173328 or at the following URL: https://www.ncbi.nlm.nih.gov/bioproject/PRJNA1173328. The other data generated in the present study may be requested from the corresponding author.

Authors' contributions

XBW, XRL and TL designed the present study. XRL, GJS, YW, TTC, PZ, TL and LL performed the experiments and acquired the data. XRL, TL, CHL and XBW analyzed the data. XRL and XBW drafted the manuscript. CHL, LL and TL revised the manuscript. XBW and XRL provided final approval of the manuscript. XRL and XBW confirmed the authenticity of all the raw data. All authors have read and approved the final manuscript.

Ethics approval and consent to participate

All experimental designs and protocols involving animals were approved by the Institutional Animals Ethics Committee at Southwest Medical University, China (approval no. 20221117-011; Luzhou, China).

Patient consent for publication

Not applicable.

Competing interests

The authors declare that they have no competing interests.

References

1. Kim SH and Fechner J: Remimazolam-current knowledge on a new intravenous benzodiazepine anesthetic agent. Korean J Anesthesiol 75: 307-315, 2022.
2. Sneyd JR and Rigby-Jones AE: Remimazolam for anaesthesia or sedation. Curr Opin Anaesthesiol 33: 506-511, 2020.
3. Lu K, Wei S, Ling W, Wei Y, Ran X, Huang H, Wang M, Wei N, Liao Y, Qin Z, *et al*: Remimazolam versus propofol for deep sedation/anaesthesia in upper gastrointestinal endoscopy in elderly patients: A multicenter, randomized controlled trial. J Clin Pharm Ther 47: 2230-2236, 2022.
4. De Hert S and Moerman A: Myocardial injury and protection related to cardiopulmonary bypass. Best Pract Res Clin Anaesthesiol 29: 137-149, 2015.
5. Cherry AD: Mitochondrial dysfunction in cardiac surgery. Anesthesiol Clin 37: 769-785, 2019.
6. Francisco J and Del Re DP: Inflammation in myocardial ischemia/reperfusion injury: Underlying mechanisms and therapeutic potential. Antioxidants (Basel) 12: 1944, 2023.
7. Ong SB, Hernández-Reséndiz S, Crespo-Avilan GE, Mukhametshina RT, Kwek XY, Cabrera-Fuentes HA and Hausenloy DJ: Inflammation following acute myocardial infarction: Multiple players, dynamic roles, and novel therapeutic opportunities. Pharmacol Ther 186: 73-87, 2018.
8. Liu Y, Li L, Wang Z, Zhang J and Zhou Z: Myocardial ischemia-reperfusion injury; molecular mechanisms and prevention. Microvasc Res 149: 104565, 2023.
9. Burgoyne JR, Mongue-Din H, Eaton P and Shah AM: Redox signaling in cardiac physiology and pathology. Circ Res 111: 1091-1106, 2012.
10. Ngo DH and Vo TS: An updated review on pharmaceutical properties of gamma-aminobutyric acid. Molecules 24: 2678, 2019.
11. Chen C, Zhou X, He J, Xie Z, Xia S and Lu G: The roles of GABA in ischemia-reperfusion injury in the central nervous system and peripheral organs. Oxid Med Cell Longev 2019: 4028394, 2019.
12. Tian J and Kaufman DL: The GABA and GABA-receptor system in inflammation, anti-tumor immune responses, and COVID-19. Biomedicines 11: 254, 2023.
13. Wang J, Zhang H, Yuan H, Chen S, Yu Y, Zhang X, Gao Z, Du H, Li W, Wang Y, *et al*: Prophylactic supplementation with lactobacillus reuteri or its metabolite GABA protects against acute ischemic cardiac injury. Adv Sci (Weinh) 11: e2307233, 2024.

14. Liu T, Lai T, Chen J, Lu Y, He F, Chen Y and Xie Y: Effect of remimazolam induction on hemodynamics in patients undergoing valve replacement surgery: A randomized, double-blind, controlled trial. Pharmacol Res Perspect 9: e00851, 2021.
15. Tang F, Yi JM, Gong HY, Lu ZY, Chen J, Fang B, Chen C and Liu ZY: Remimazolam benzenesulfonate anesthesia effectiveness in cardiac surgery patients under general anesthesia. World J Clin Cases 9: 10595-10603, 2021.
16. Wang Z, Huang S, Sheng Y, Peng X, Liu H, Jin N, Cai J, Shu Y, Li T, Li P, *et al*: Topiramate modulates post-infarction inflammation primarily by targeting monocytes or macrophages. Cardiovasc Res 113: 475-487, 2017.
17. Cai W, Liu L, Shi X, Liu Y, Wang J, Fang X, Chen Z, Ai D, Zhu Y and Zhang X: Alox15/15-HpETE aggravates myocardial ischemia-reperfusion injury by promoting cardiomyocyte ferroptosis. Circulation 147: 1444-1460, 2023.
18. Gao E, Lei YH, Shang X, Huang ZM, Zuo L, Boucher M, Fan Q, Chuprun JK, Ma XL and Koch WJ: A novel and efficient model of coronary artery ligation and myocardial infarction in the mouse. Circ Res 107: 1445-1453, 2010.
19. Tan XQ, Cheng XL, Zhang L, Wu BW, Liu QH, Meng J, Xu HY and Cao JM: Multi-walled carbon nanotubes impair Kv4.2/4.3 channel activities, delay membrane repolarization and induce bradyarrhythmias in the rat. PLoS One 9: e101545, 2014.
20. Tang L, Sim I, Moqbel S and Wu L: Dapansutrile ameliorated chondrocyte inflammation and osteoarthritis through suppression of MAPK signaling pathway. Hum Exp Toxicol 41: 9603271221145401, 2022.
21. Livak KJ and Schmittgen TD: Analysis of relative gene expression data using real-time quantitative PCR and the 2(-Delta Delta C(T)) method. Methods 25: 402-408, 2001.
22. Chen R, Zhang H, Tang B, Luo Y, Yang Y, Zhong X, Chen S, Xu X, Huang S and Liu C: Macrophages in cardiovascular diseases: Molecular mechanisms and therapeutic targets. Signal Transduct Target Ther 9: 130, 2024.
23. Chong AJ, Pohlman TH, Hampton CR, Shimamoto A, Mackman N and Verrier ED: Tissue factor and thrombin mediate myocardial ischemia-reperfusion injury. Ann Thorac Surg 75: S649-S655, 2003.
24. Toldo S and Abbate A: The NLRP3 inflammasome in acute myocardial infarction. Nat Rev Cardiol 15: 203-214, 2018.
25. Hu Q, Liu X, Wen C, Li D and Lei X: Remimazolam: An updated review of a new sedative and anaesthetic. Drug Des Devel Ther 16: 3957-3974, 2022.
26. Antonik LJ, Goldwater DR, Kilpatrick GJ, Tilbrook GS and Borkett KM: A placebo- and midazolam-controlled phase I single ascending-dose study evaluating the safety, pharmacokinetics, and pharmacodynamics of remimazolam (CNS 7056): Part I. Safety, efficacy, and basic pharmacokinetics. Anesth Analg 115: 274-283, 2012.
27. Kilpatrick GJ: Remimazolam: Non-clinical and clinical profile of a new sedative/anesthetic agent. Front Pharmacol 12: 690875, 2021.
28. He J, Liu D, Zhao L, Zhou D, Rong J, Zhang L and Xia Z: Myocardial ischemia/reperfusion injury: Mechanisms of injury and implications for management (Review). Exp Ther Med 23: 430, 2022.
29. Heusch G: Myocardial ischemia/reperfusion: Translational pathophysiology of ischemic heart disease. Med 5: 10-31, 2024.
30. Gunata M and Parlakpinar H: A review of myocardial ischaemia/reperfusion injury: Pathophysiology, experimental models, biomarkers, genetics and pharmacological treatment. Cell Biochem Funct 39: 190-217, 2021.
31. Wu L, Zhao H, Wang T, Pac-Soo C and Ma D: Cellular signaling pathways and molecular mechanisms involving inhalational anesthetics-induced organoprotection. J Anesth 28: 740-758, 2014.
32. Ferrando C, Soro M and Belda FJ: Protection strategies during cardiopulmonary bypass: Ventilation, anesthetics and oxygen. Curr Opin Anaesthesiol 28: 73-80, 2015.
33. Li S, Lei Z, Yang X, Zhao M, Hou Y, Wang D, Tang S, Li J and Yu J: Propofol protects myocardium from ischemia/reperfusion injury by inhibiting ferroptosis through the AKT/p53 signaling pathway. Front Pharmacol 13: 841410, 2022.
34. Eroglu A: The effect of intravenous anesthetics on ischemia-reperfusion injury. Biomed Res Int 2014: 821513, 2014.
35. Zhang GR, Peng CM, Liu ZZ and Leng YF: The effect of dexmedetomidine on myocardial ischemia/reperfusion injury in patients undergoing cardiac surgery with cardiopulmonary bypass: A meta-analysis. Eur Rev Med Pharmacol Sci 25: 7409-7417, 2021.
36. Sneyd JR, Absalom AR, Barends CRM and Jones JB: Hypotension during propofol sedation for colonoscopy: A retrospective exploratory analysis and meta-analysis. Br J Anaesth 128: 610-622, 2022.
37. Kim KM: Remimazolam: Pharmacological characteristics and clinical applications in anesthesiology. Anesth Pain Med (Seoul) 17: 1-11, 2022.
38. Algoet M, Janssens S, Himmelreich U, Gsell W, Pusovnik M, Van den Eynde J and Oosterlinck W: Myocardial ischemia-reperfusion injury and the influence of inflammation. Trends Cardiovasc Med 33: 357-366, 2023.
39. Xiang M, Lu Y, Xin L, Gao J, Shang C, Jiang Z, Lin H, Fang X, Qu Y, Wang Y, *et al*: Role of oxidative stress in reperfusion following myocardial ischemia and its treatments. Oxid Med Cell Longev 2021: 6614009, 2021.
40. Liu Y, Li X, Sun T, Li T and Li Q: Pyroptosis in myocardial ischemia/reperfusion and its therapeutic implications. Eur J Pharmacol 971: 176464, 2024.
41. Toldo S, Mauro AG, Cutter Z and Abbate A: Inflammasome, pyroptosis, and cytokines in myocardial ischemia-reperfusion injury. Am J Physiol Heart Circ Physiol 315: H1553-H1568, 2018.
42. Xia Y, He F, Wu X, Tan B, Chen S, Liao Y, Qi M, Chen S, Peng Y, Yin Y and Ren W: GABA transporter sustains IL-1β production in macrophages. Sci Adv 7: eabe9274, 2021.
43. Bu J, Huang S, Wang J, Xia T, Liu H, You Y, Wang Z and Liu K: The $GABA_A$ receptor influences pressure overload-induced heart failure by modulating macrophages in mice. Front Immunol 12: 670153, 2021.
44. Yi S, Tao X, Wang Y, Cao Q, Zhou Z and Wang S: Effects of propofol on macrophage activation and function in diseases. Front Pharmacol 13: 964771, 2022.
45. Liu XR, Cao L, Li T, Chen LL, Yu YY, Huang WJ, Liu L and Tan XQ: Propofol attenuates H_2O_2-induced oxidative stress and apoptosis via the mitochondria- and ER-medicated pathways in neonatal rat cardiomyocytes. Apoptosis 22: 639-646, 2017.